

Null Detection in Shear-Wave Splitting Measurements

by Andreas Wüstefeld and Götz Bokelmann

Abstract Shear-wave splitting measurements are widely used to analyze orientations of anisotropy. We compare two different shear-wave splitting techniques, which are generally assumed to give similar results. Using a synthetic test, which covers the whole backazimuthal range, we find characteristic differences, however, in fast-axis and delay-time estimates near Null directions between the rotation correlation and the minimum energy method. We show how this difference can be used to identify Null measurements and to determine the quality of the result. This technique is then applied to teleseismic events recorded at station LVZ in northern Scandinavia, for which our method constrains the fast-axis azimuth to be 15° and the delay time 1.1 sec.

Online material: Additional comparisons between the RC and SC techniques.

Introduction

Understanding seismic anisotropy can help to constrain present and past deformation processes within the Earth. If this deformation occurs in the upper mantle, the accompanying strain tends to align anisotropic minerals, especially olivine (Nicolas and Christensen, 1987). Seismic anisotropy means that a wave travels faster in one direction than in a different one. Shear waves passing through such a medium are split into two orthogonal polarized components that travel at different velocities. The one polarized parallel to the fast direction leads the orthogonal component. The delay time between those two components is proportional to the thickness of the anisotropic layer and the strength of anisotropy.

Analyzing teleseismic shear-wave splitting has become a widely adopted technique for detecting such anisotropic structures in the Earth's crust and mantle. Two complementary types of techniques exist for estimating the two splitting parameters, anisotropic fast axis Φ and delay time δt . The first type (multievent techniques) utilizes simultaneously a set of records coming from different azimuths. Vinnik *et al.* (1989) propose to stack the transverse components with weights depending on azimuths. Chevrot (2000) projects the amplitudes of transverse components onto the amplitudes of the time derivatives of radial components to obtain the so-called splitting vector. Phase and amplitude of the best-fitting curve then give fast axis and delay time, respectively.

The second type of techniques determines the splitting parameters on a per-event basis (Bowman and Ando, 1987; Silver and Chan, 1991; Menke and Levin, 2003). A grid search is performed for the set of parameters that best remove the effect of splitting. Different measures for “best removal” exist.

We will focus here on the second type (per-event meth-

ods) and will show that they behave rather differently close to “Null” directions. Such Null measurements occur either if the wave propagates through an isotropic medium or if the initial polarization coincides with either the fast or the slow axis. In these cases the incoming shear wave is not split (Savage, 1999). It is important, therefore, to identify such so-called Null measurements. Indeed, Null measurements are often treated separately (Silver and Chan, 1991; Barruol *et al.*, 1997; Fouch *et al.*, 2000; Currie *et al.*, 2004) or even neglected in shear-wave splitting studies. In particular, Nulls do not constrain the delay time and the estimated fast axis corresponds either to the (real) fast or slow axis. In the absence of anisotropy the estimated fast axis simply reflects the initial polarization, which for *SKS* waves usually corresponds to the backazimuth. Therefore, the backazimuthal distribution of Nulls may reflect not only the geometry, but the strength of anisotropy: media with strong anisotropy display Nulls only from four small, distinct ranges of backazimuths, whereas purely isotropic media are characterized by Nulls from all backazimuths. Small splitting delay times may also be observed in weak anisotropic media or in (strongly) anisotropic media with lateral and/or vertical variations over short distances (Saltzer *et al.*, 2000). Such cases may thus resemble a Null. Typically, the identification of Nulls and non-Nulls is done by the seismologist, based on criteria including the ellipticity of the particle motion before correction, linearity of particle motion after correction, the signal-to-noise ratio on transverse component (SNR_T), and the waveform coherence in the fast-slow system (Barruol *et al.*, 1997). Such approach has its limits for near-Nulls, where a consistent and reproducible classification is difficult.

Here, we present a Null identification criterion based on differences in splitting parameter estimates of two tech-

niques. We apply this to synthetic and real data. Such an objective numerical criterion is an important step toward a fully automated splitting analysis. Automation becomes more important with the rapid increase of seismic data over the past as well as in future years (Teanby *et al.*, 2003).

Single-Event Techniques

When propagating through an anisotropic layer, an incident S wave is split into two quasi-shear waves, polarized in the fast and the slow direction. The difference in velocity leads to an accumulating delay time while propagating through the medium (see Savage, 1999, for a review). Single-event shear-wave splitting techniques remove the effect of splitting by a grid search for the splitting parameters Φ (fast axis) and δt (delay time) that best remove the effect of splitting from the seismograms.

Assuming an incident wave \mathbf{u}_0 (with radial component u_R and transverse component u_T), the splitting process can be described as $\tilde{\mathbf{u}}(\omega) = \mathbf{R}^{-1} \mathbf{D} \mathbf{R} \mathbf{u}_0(\omega)$, (Silver and Chan, 1991) that is, by a combination of a rotation of \mathbf{u}_0 about angle α between backazimuth, ψ , and fast direction Φ_{fast}

$$\mathbf{R} = \begin{bmatrix} \cos \alpha & -\sin \alpha \\ \sin \alpha & \cos \alpha \end{bmatrix} \quad (1)$$

and simultaneously a time delay δt

$$\mathbf{D} = \begin{bmatrix} e^{i\omega\delta t/2} & 0 \\ 0 & e^{-i\omega\delta t/2} \end{bmatrix}. \quad (2)$$

The resulting radial and transverse displacements \tilde{u}_R and \tilde{u}_T in the time domain after the splitting of a noise-free initial waveform $w(t)$ are thus given by

$$\begin{aligned} \tilde{u}_R(\alpha, t) &= w(t + \delta t/2) \cos^2 \alpha + w(t - \delta t/2) \sin^2 \alpha \\ \tilde{u}_T(\alpha, t) &= -\frac{1}{2} [w(t - \delta t/2) - w(t + \delta t/2)] \sin 2\alpha \end{aligned} \quad (3)$$

For the SKS and $SKKS$ phases that are usually studied with this technique, the initial polarization of $w(t)$ is in general in the radial direction. α corresponds therefore to the angle between the radial direction and the fast polarization axis. Silver and Chan (1991) demonstrated that the splitting parameters can be found from the time-domain covariance matrix of the horizontal particle motion

$$C_{ij}(\alpha, \delta t) = \int_{-\infty}^{\infty} \tilde{u}_i(\alpha, t) \tilde{u}_j(\alpha, t - \delta t) dt; \quad (4)$$

$i, j = \text{Radial, Transverse.}$

Two different techniques of this single-event approach exist. The first is the rotation-correlation technique (RC), which rotates the seismograms into a test coordinate system and

searches for the direction α where the cross-correlation coefficient is maximum thus returning the splitting parameter estimates Φ_{RC} and δt_{RC} (Fukao, 1984; Bowman and Ando, 1987). This technique can be visualized as searching for the splitting parameter combination $(\alpha, \delta t)$ that maximizes the similarity in the nonnormalized pulse shapes of the two corrected seismogram components. The second technique considered here searches for the most singular covariance matrix based on its eigenvalues λ_1 and λ_2 . Silver and Chan (1991) emphasize the similarity of a variety of such measures such as maximizing λ_1 or λ_1/λ_2 and minimizing λ_2 or $\lambda_1 * \lambda_2$. A special case of this technique can be applied if initial wave polarization is known (as with SKS , $SKKS$) and if the noise level is low. In this case the energy on the transverse component

$$E_{\text{trans}} = \int_{-\infty}^{\infty} \tilde{u}_T^2(t) dt \quad (5)$$

after reversing the splitting can be minimized. In the following we refer to this technique as SC, with the corresponding splitting parameter estimates Φ_{SC} and δt_{SC} . All of these single-event techniques rely on a good signal-to-noise ratio (Restivo and Helffrich, 1998). Another limit is the assumption of transverse isotropy and one layer of horizontal axis of symmetry and thus only provides apparent splitting parameters. This is commonly compensated by analyzing the variation of these apparent parameters with backazimuth (e.g., Özalaybey and Savage, 1994; Brechner *et al.*, 1998).

Synthetic Test

We first compare the RC with the SC technique in a synthetic test. Figure 1 displays an example result for both techniques for a model that consists of a single anisotropic layer with input fast axes of $\Phi_{\text{in}} = 0^\circ$ and splitting delay time $\delta t_{\text{in}} = 1.3$ sec at a backazimuth of 10° . Our input wavelet $w(t)$ is the first derivative of a Gauss-type function

$$w(t) = -2 \frac{t - t_0}{\sigma} * \exp - \left(\frac{t - t_0}{\sigma} \right)^2. \quad (6)$$

For $\sigma = 3$ the dominant period is ~ 8 sec. This wavelet was then used in the splitting equations (3), given by Silver and Chan (1991), to calculate the radial and transverse components for the given set of splitting parameters $(\Phi, \delta t)$. We added Gaussian-distributed noise, bandpass-filtered between 0.02 and 1 Hz, and determined the SNR as

$$\begin{aligned} \text{SNR}_R &= \max(|\tilde{u}_R|) / 2\sigma_T \\ \text{SNR}_T &= \max(|\tilde{u}_T|) / 2\sigma_T \end{aligned} \quad (7)$$

For SNR_R this is similar to Restivo and Helffrich (1998),

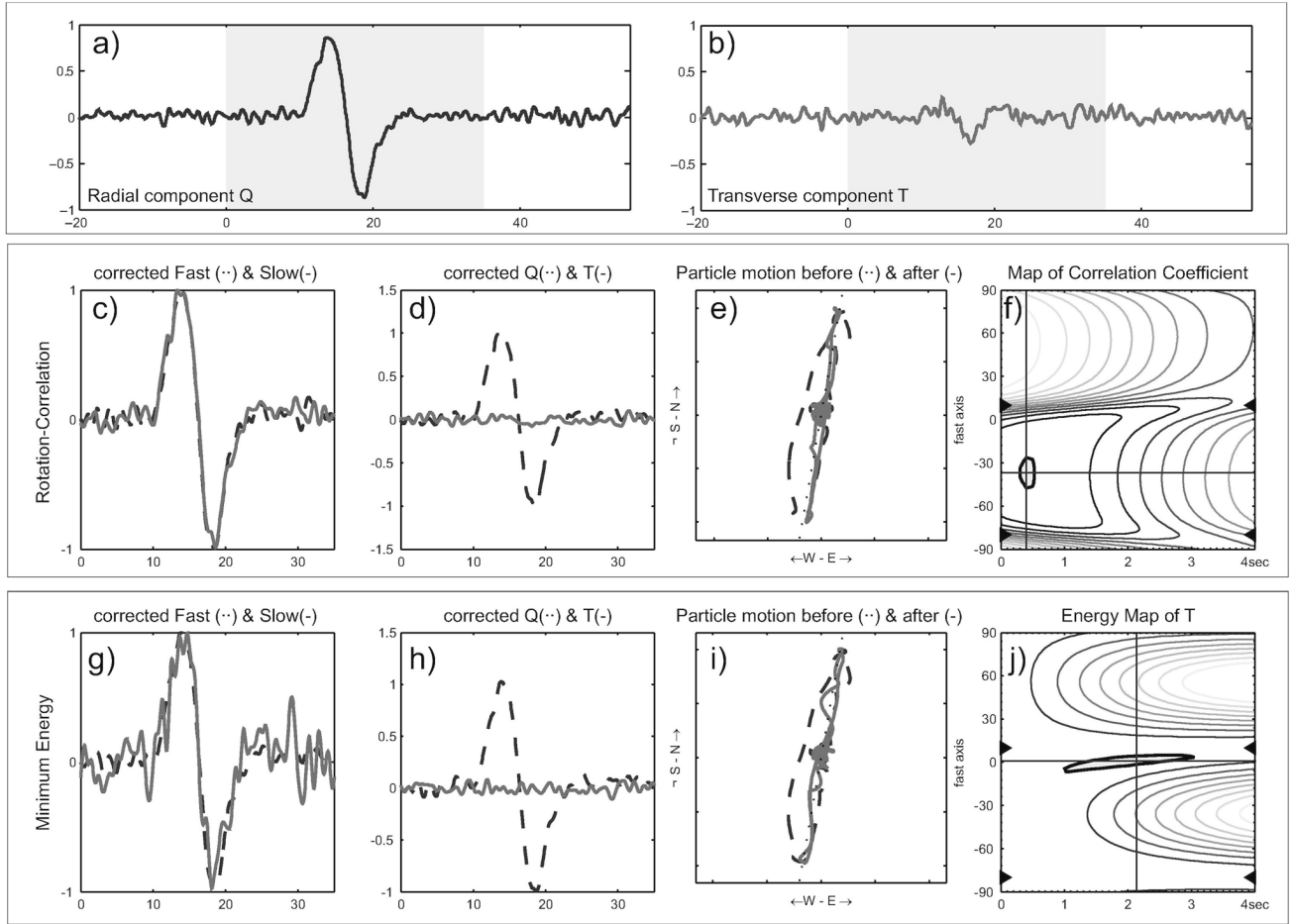


Figure 1. Synthetic splitting example with fast axis at 0° , delay time 1.3 sec, and backazimuth 10° (“near-Null case”) for a SNR_R of 15. Upper panel displays the initial seismograms: radial (a) and transverse (b) component, both bandpass filtered between 0.02 and 1 Hz. The shaded area represents the selected time window. The center panel displays the results for the RC technique: normalized components after rotation in RC-anisotropy system (c); radial (Q) and transverse (T) seismogram components after RC correction (d); particle motion before and after RC correction (e); map of correlation (f). Lower panel displays the results for the minimum energy (SC) technique: normalized components after rotation in SC anisotropy system (g); corrected (SC) radial and transverse seismogram component (h); SC particle motion before and after correction (i); map of minimum energy on transverse component (j).

where the “signal” level is the maximum amplitude of the radial component before correction. The 2σ envelope of the corrected transverse component gives the noise level. For example, in Figure 1 we obtain an SNR_R of 15 and SNR_T of 3, respectively (compare with the seismograms in the first panel on the top).

The backazimuth for the example in Figure 1 is 10° and it thus constitutes a near-Null measurement. Note that the two techniques produce different sets of optimum splitting parameter estimates. Although the optimum for SC recovers approximately the correct solution, RC deviates significantly. In the following, we will analyze the performance of the two techniques for the whole range of backazimuths.

Figure 2 displays the splitting parameter estimates (fast axis Φ_{RC} and Φ_{SC} and delay times δt_{RC} and δt_{SC}) for different

backazimuths ψ . This synthetic test shows that both techniques give correct values if backazimuths are sufficiently far away from fast or slow directions. Near these Null directions there are characteristic deviations, especially for the RC technique. Values of δt_{RC} diminish systematically, whereas Φ_{RC} shows deviations of about 45° near Null directions. Perhaps surprisingly, the Φ_{RC} lies along lines that indicate backazimuth $\pm 45^\circ$. The explanation of this behavior is that the RC technique seeks for maximum correlation between the two horizontal components Q (radial) and T (transverse). However, in a Null case the energy on T is negligible and for any test fast axis F

$$\begin{bmatrix} F \\ S \end{bmatrix} = \begin{bmatrix} \cos \Phi & -\sin \Phi \\ \sin \Phi & \cos \Phi \end{bmatrix} \cdot \begin{bmatrix} Q \\ T \end{bmatrix} = \begin{bmatrix} Q \cos \Phi \\ Q \sin \Phi \end{bmatrix} \quad (8)$$

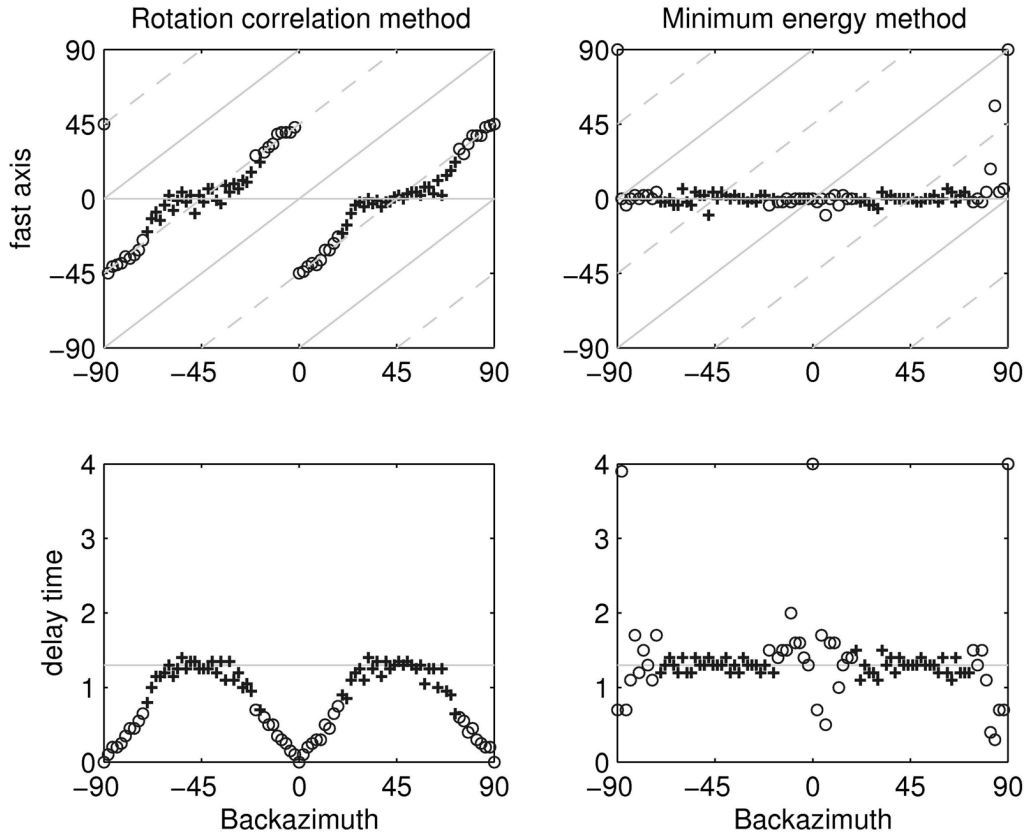


Figure 2. Synthetic test at $\text{SNR}_R = 15$ for the RC technique (left) and the minimum energy technique (SC). Upper panels show the resulting fast axes at different backazimuths; lower panels show the resulting delay time estimates. Input values $\Phi_{\text{in}} = 0^\circ$ and $dt_{\text{in}} = 1.3$ sec are indicated by horizontal lines. The SC technique yields stable estimates for a wide range of backazimuths. For lower SNR_R and/or smaller delay times (see the supplement in the online edition of BSSA) the RC technique differs even more from the input values. Automatically detected good Nulls are marked as circles; near Nulls are squares. Good splitting results are marked as plus signs, and fair results are crosses. Poor results are indicated as dots.

the test slow axis S gains its energy only from the Q -component. The waveform on both F and S is identical with the Q -component waveform with no delay time. Consequently, the F - S cross-correlation yields its maximum for $\Phi = 45^\circ$, where $\sin(\Phi) = \cos(\Phi)$ (anticorrelated for $\Phi = -45^\circ$). For this reason the fast azimuth estimated by the RC technique is off by $\pm 45^\circ$ near Null directions from the true fast-azimuth direction, whereas δt_{RC} tends toward zero.

In comparison, the SC technique is relatively stable except for large scatter near Nulls. Here, the SC fast-axis estimate, Φ_{SC} , deviates around $\pm n \cdot 90^\circ$ from the input fast axis and the delay time estimates δt_{SC} scatter and often reach the maximum search values (here, 4 sec). This results from energy maps with elongated confidence areas along the time axis (Fig. 1j), probably in conjunction with signal-generated noise. In agreement with Restivo and Helffrich (1998), it appears that δt_{SC} typically is reliable if the backazimuth differs more than 15° from a Null direction. We tested this result for different input delay times and noise levels (see the supplement in the online edition of BSSA). The width

of the plateau of correct Φ_{RC} and δt_{RC} estimates (Fig. 2) is a function of both input delay time and SNR_T . Higher delay times and/or higher SNR_T result in wider plateaus. In contrast, for small input delay times and low SNR_T the backazimuthal range over which Φ_{RC} falls onto the $\pm 45^\circ$ lines from the backazimuth (dotted in Fig. 2) becomes wider, until it eventually encompasses the whole backazimuth range. On the other hand, SC shows scatter for a larger range but no systematic deviation.

Comparing the results of the two techniques can thus help to detect Null measurements. For a Null measurement, the angular difference between the two techniques is

$$\Delta\Phi = \Phi_{\text{SC}} - \Phi_{\text{RC}} \approx n \cdot 45^\circ, \quad (9)$$

where n is a positive or negative integer. For backazimuths deviating from a Null direction, the difference in fast-axis estimates decreases rapidly depending on noise level and input delay time. Figure 2 displays that for an SNR_R of 15 a near-Null can be clearly identified as having, in general,

$|\Delta\Phi| \geq 45^\circ/2$. Near Null directions the RC delay times are biased toward zero. The backazimuth with minimum δt_{RC} is thus a further indicator of a Null direction (Fig. 2). Teleseismic non-Null measurements thus require the following criteria: (1) the ratio of delay-time estimates from the two techniques ($\rho = \delta t_{RC}/\delta t_{SC}$) is larger than 0.7 and (2) the difference between the fast-axis estimates of both techniques, $|\Delta\Phi|$, is smaller than 22.5° . Events with $\text{SNR}_T < 3$ are classified as Nulls.

Wolfe and Silver (1998) remark that waveforms containing energy at periods (T) less than ten times the splitting delays are required to obtain a good measurement. However, the arc-shaped pattern of δt_{RC} persists for smaller delay times. Thus, the characteristics of the backazimuthal plots (as discussed previously) can provide valuable additional information on the anisotropic parameters.

Detecting Nulls using a data-based criterion provides three advantages. First, it eliminates subjective measures such as evaluating initial particle motion and resulting energy map. Second, by varying the threshold values of $\Delta\Phi$ and ρ , the user can change the sensitivity of Null detection. And third, the separation of Nulls is necessary for future automated splitting approaches. Because available data in-

crease rapidly, the automation of the splitting process is a desirable goal in future applications and procedures.

Quality Determination

We furthermore use the difference between results from the two techniques as a quality measure of the estimation. Again, such a data-based measure is more objective than visual quality measures based on seismogram shape and linearization (Barruol *et al.*, 1997). In Figure 3 we compare, similar to Levin *et al.* (2004), both techniques by plotting the difference of fast-axis estimates ($|\Delta\Phi|$) versus ratio of delay times ($\rho = \delta t_{RC}/\delta t_{SC}$) of synthetic seismograms.

Based on the synthetic measurements (Fig. 2), we define as good splitting measurements if $0.8 < \rho < 1.1$ and $\Delta\Phi < 8^\circ$ and fair splitting if $0.7 < \rho < 1.2$ and $\Delta\Phi < 15^\circ$. Null measurements are identified as differences in fast-axis estimates of about 45° and a small delay-time ratio ρ . Near the true Null directions the SC fast axis estimates are more robust than the RC technique (Fig. 2). A differentiation between Nulls and near-Nulls is useful in the interpretation of backazimuthal plots (Fig. 2). Good Nulls are characterized by a small time ratio ($0 < \rho < 0.2$) and, following equation

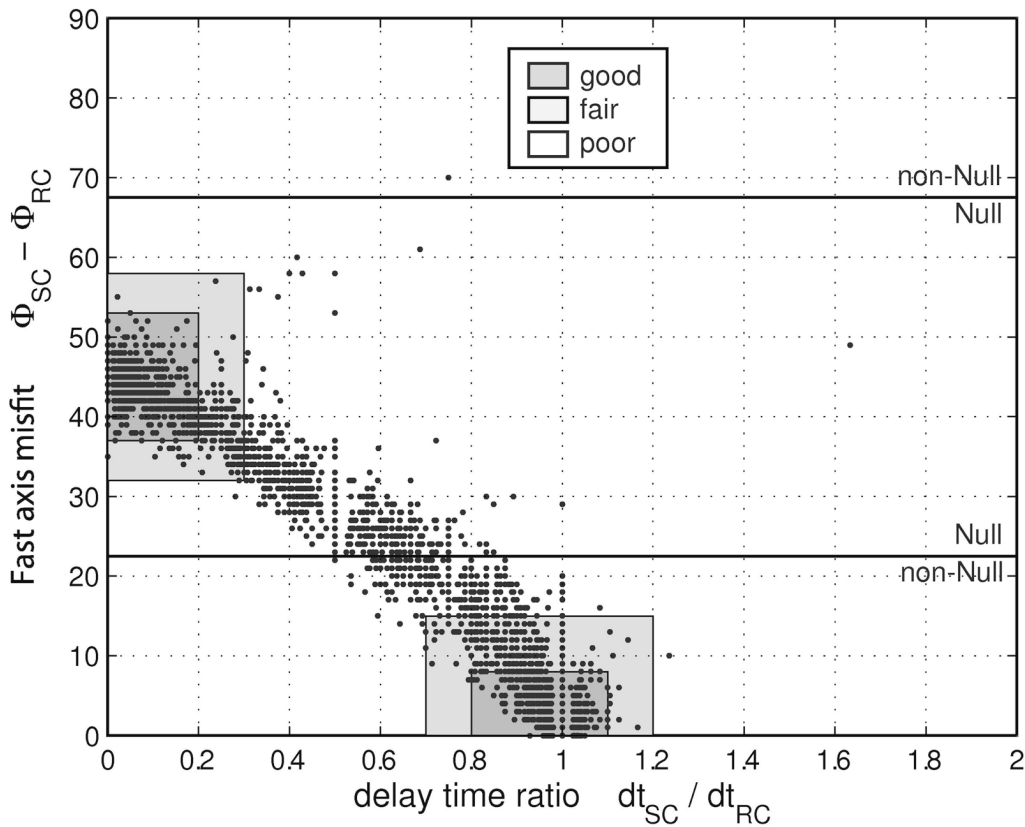


Figure 3. Misfit of delay-time and fast-axis estimates between RC and the SC techniques calculated for 3185 synthetic seismograms at five different SNR_R values between 3 and 30 and seven input delay times between 0 and 2 sec from all backazimuths. The Null criterion helps to identify Null measurements and at the same time gives a quality attribute. Fair Null measurements are equivalent to near, Nulls.

(9), a difference in fast axis estimate close to 45° , that is $37^\circ < \Delta\Phi < 53^\circ$. Near-Null measurements can be classified by $0 < \rho < 0.3$ and $32^\circ < \Delta\Phi < 58^\circ$. Remaining measurements are to be considered as poor quality (see Fig. 3 for further illustration).

Real Data

We apply our Null criterion to the shear-wave splitting measurements of station LVZ in northern Scandinavia. The analyzed earthquakes ($M_w \geq 6$) occurred between December 1992 and December 2005. The data were processed by using the SplitLab environment (A. Wüstefeld *et al.*, unpublished manuscript, 2006). This allows us to analyze events efficiently and to calculate simultaneously both the RC and SC technique. We mostly used raw data or, where necessary, applied third-order Butterworth bandpass filters with upper-corner frequencies down to 0.2 Hz. Most usable events have backazimuths between 45° and 100° . Such sparse backazimuthal coverage is unfortunately the case for many splitting

analyses, and we aim to extract the maximum information about the splitting parameters from these sparse distributions.

In total we analyzed 37 SKS phases from a wide range of backazimuths (Fig. 4). Many results resemble Null characteristics by showing low energy on the initial transverse component, elongated to linear initial particle motion and a typical energy plot. Such characteristics can be replicated in synthetic seismograms with near-Null parameters, that is, when the fast axis deviates less than 20° from backazimuth (Fig. 1). The average fast axis of the good events, as detected automatically and manually, is 14.3° and 14.7° for the SC and RC technique, respectively. Such orientation implies Nulls at backazimuths of approximately 15° , 105° , 195° , and 285° and favorable backazimuths for splitting measurements in between. Indeed, good and fair splitting measurements are found in backazimuthal ranges between 50° and 70° (Table 1 and Fig. 4), where the energy on the transverse component is expected to reach maximum possible values (see equation 3) and the splitting can be inverted most reliably.

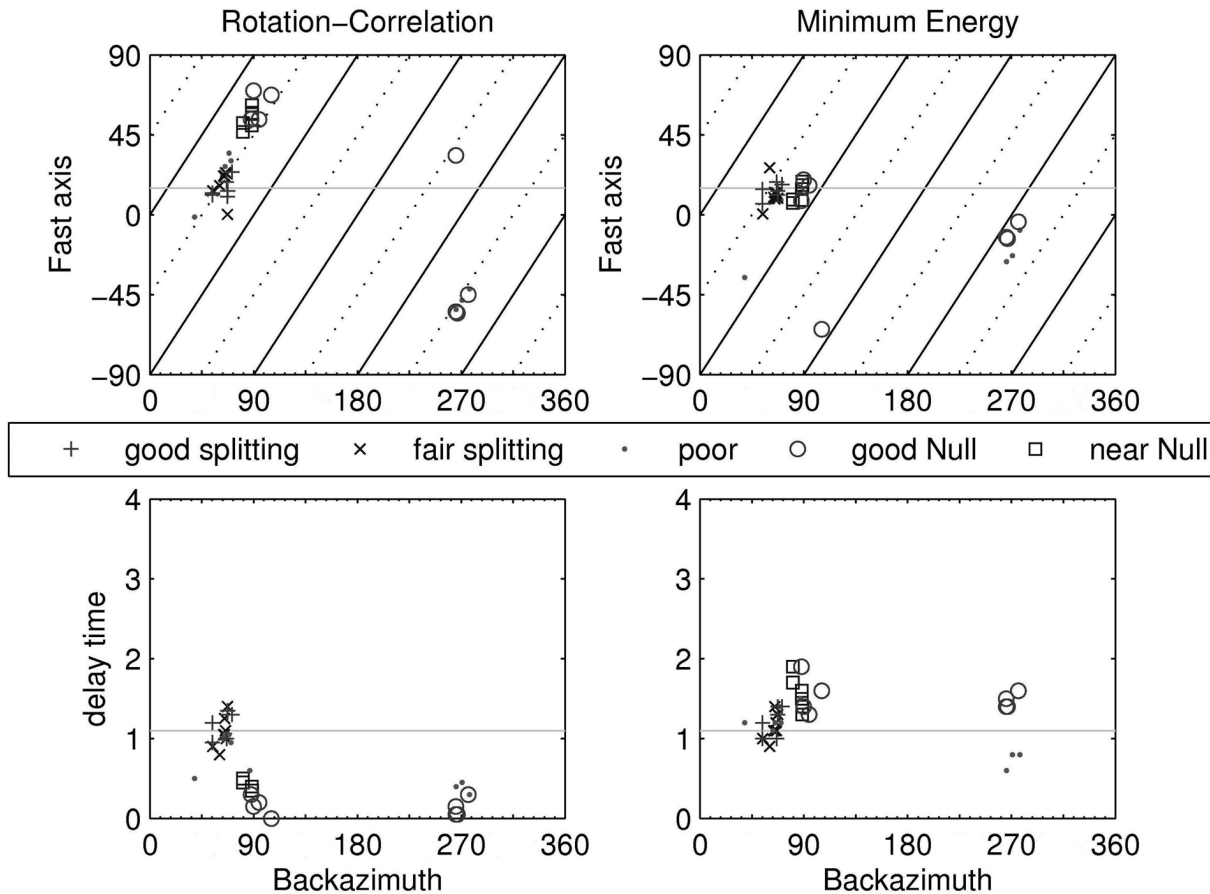


Figure 4. Shear-wave splitting estimates from 33 good and fair measurements from station LVZ. The upper panels display fast-axis estimates for RC and SC methods. Note that many RC estimates are situated near the dotted lines that indicate 45° . The lower panels display the delay-time estimates. The solid horizontal lines indicate our interpretation of the LVZ with fast axis at 15° and 1.1-sec delay time, based on the mean of the good splitting measurements.

Table 1
Good Events of Station LVZ as Detected Automatically

Date	Lat	Long	Bazi*	Φ_{SC}	Φ_{RC}	δt_{SC}	δt_{RC}	SNR_{SC}^\dagger	$corr_{RC}^\ddagger$
01-Oct-1994	-17.75	167.63	55.1	19.1	13.1	0.8	0.8	5.85	0.89
17-Mar-1996	-14.7	167.3	54.3	14.3	12.3	1.0	1.0	9.55	0.93
05-Apr-1997	-6.49	147.41	71.1	17.1	24.1	1.4	1.3	6.16	0.88
06-Feb-1999	-12.85	166.7	54.2	6.2	11.2	1.2	1.2	10.43	0.97
10-May-1999	-5.16	150.88	67.3	11.3	10.3	1.3	1.3	5.70	0.87
06-Feb-2000	-5.84	150.88	67.5	13.5	13.5	1.4	1.4	9.33	0.91
18-Nov-2000	-5.23	151.77	66.5	18.5	18.5	1.0	1.0	5.74	0.90

*Bazi, backazimuth

$^\dagger SNR_{SC}$, signal-to-noise ratio of the SC technique.

$^\ddagger corr_{RC}$, correlation coefficient of the RC technique.

Also in good agreement are the detected Nulls at backazimuths between 80° and 110° and at about 270° .

Simultaneously, RC delay times systematically tend to smaller values between backazimuths of 80° and 110° , mimicking the trapezoidal shape in the synthetic RC delay times (Fig. 2). Mean delay time estimates of good SC and RC are 1.2 and 1.1 sec. respectively.

Discussion and Conclusions

We have presented a novel criterion for identifying Null measurements in shear-wave splitting data based on two independent and commonly used splitting techniques. The two techniques behave very differently near Null directions, where the RC technique systematically fails to extract the correct values both for the fast-axis azimuth Φ_{RC} and delay time δt_{RC} . That technique should therefore not be used as a “stand-alone” technique. On the other hand, the comparison of the two techniques is valuable for finding Null events. The backazimuths of Nulls ambiguously indicates either fast or slow direction. Thus, a Null measurement yields limited, yet important, constraints on anisotropy orientation, especially if the backazimuthal coverage of the station is only sparse. Furthermore, Nulls from a wide range of backazimuths indicate either the lack of (azimuthal) anisotropy or weak anisotropy, at the limit of detection. Restivo and Helffrich (1998) analyzed the splitting procedure for effects of noise. They conclude that for small splitting filtering does not necessarily result in more confident estimates of splitting parameters, since narrow bandpass filters lead to apparent Null measurements. For SNR above 5 our criterion detects Null measurements and classifies near-Nulls. Good events can still be obtained but only for exceptionally good SNR or with backazimuths far away oriented with respect to the anisotropy axes (where the transverse amplitude is larger; see equation 3).

The comparison of the two shear-wave splitting techniques allows assigning a quality to single measurements (Fig. 1). Furthermore, the joint two-technique analysis of all measurements (Fig. 2) yields characteristic variations of splitting parameter estimates with backazimuth. This varia-

tion can be used to extract the maximum information from the data, and to decide whether a more complex anisotropy than a single layer needs to be invoked to explain the observations. The practical steps for this should be: first, assume a single-layer case with the most probable fast direction based on the good measurements. Second, verify that Nulls measurements occur near the corresponding Null directions in the backazimuth plot (Fig. 4). In the vicinity of these Null directions, the splitting parameter estimates Φ_{SC} and δt_{SC} should show a larger scatter with a tendency toward large delays. For δt_{RC} we expect to find an arc-shaped variation with backazimuth that should have its minimums near the assumed Null directions. If these conditions are met, a one-layer case can reasonably explain the observations. On the other hand, good events that deviate from these predictions may require more complex anisotropy (multilayer case or dipping layer). Applied to station LVZ in northern Scandinavia, we were thus able to comfortably characterize the anisotropy by a single anisotropic layer with a fast axis oriented at 15° and a delay time of 1.1 sec.

References

- Barruol, G., P. G. Silver, and A. Vauchez (1997). Seismic anisotropy in the eastern US: Deep structure of a complex continental plate, *J. Geophys. Res.* **102**, no. B4, 8329–8348.
- Bowman, J. R., and M. Ando (1987). Shear-wave splitting in the upper-mantle wedge above the Tonga subduction zone, *Geophys. J. R. Astr. Soc.* **88**, 25–41.
- Brechner, S., K. Klinge, F. Krüger, and T. Plenefisch (1998). Backazimuthal variations of splitting parameters of teleseismic SKS phases observed at the broadband stations in Germany, *Pure Appl. Geophys.* **151**, 305–331.
- Chevrot, S. (2000). Multichannel analysis of shear wave splitting, *J. Geophys. Res.* **105**, no. B9, 21,579–21,590.
- Currie, C. A., J. F. Cassidy, R. D. Hyndman, and M. G. Bostock (2004). Shear wave anisotropy beneath the Cascadia subduction zone and western North American Craton, *Geophys. J. Int.* **157**, 341–353.
- Fouch, M. J., K. M. Fischer, E. M. Parmentier, M. E. Wysession, and T. J. Clarke (2000). Shear wave splitting, continental keels, and patterns of mantle flow, *J. Geophys. Res.* **105**, no. B3, 6255–6275.
- Fukao, Y. (1984). Evidence from core-reflected shear waves for anisotropy in the earth’s mantle, *Nature* **309**, 5970, 695.
- Levin, V., D. Droznin, J. Park, and E. Gordeev (2004). Detailed mapping

- of seismic anisotropy with local shear waves in southeastern Kamchatka, *Geophys. J. Int.* **158**, no. 3, 1009–1023.
- Menke, W., and V. Levin (2003). The cross-convolution method for interpreting SKS splitting observations, with application to one and two-layer anisotropic earth models, *Geophys. J. Int.* **154**, no. 2, 379–392.
- Nicolas, A., and N. I. Christensen (1987). Formation of anisotropy in upper mantle peridotites: a review, in *Composition Structure and Dynamics of the Lithosphere Asthenosphere System*, K. Fuchs and C. Froideveaux (Editors), American Geophysical Union, Washington, D.C., 111–123.
- Ozalaybey, S., and M. K. Savage (1994). Double-layer anisotropy resolved from S phases, *Geophys. J. Int.* **117**, 653–664.
- Restivo, A., and G. Helffrich (1999). Teleseismic shear wave splitting measurements in noisy environments, *Geophys. J. Int.* **137**, no. 3, 821–830.
- Saltzer, R. L., J. B. Gaherty, and T. H. Jordan (2000). How are vertical shear wave splitting measurements affected by variations in the orientation of azimuthal anisotropy with depth? *Geophys. J. Int.* **141**, 374–390.
- Savage, M. K. (1999). Seismic anisotropy and mantle deformation: what have we learned from shear wave splitting, *Rev. Geophys.* **37**, 69–106.
- Silver, P. G., and W. W. Chan (1991). Shear wave splitting and subcontinental mantle deformation, *J. Geophys. Res.* **96**, no. B10, 16,429–16,454.
- Teanby, N., J. M. Kendall, and M. van der Baan (2003). Automation of shear-wave splitting measurements using cluster analysis, *Bull. Seism. Soc. Am.* **94**, 453–463.
- Vinnik, L. P., V. Farra, and B. Romaniwicz (1989). Azimuthal anisotropy in the earth from observations of SKS at GEOSCOPE and NARS broadband stations, *Bull. Seism. Soc. Am.* **79**, no. 5, 1542–1558.
- Wolfe, C. J., and P. G. Silver (1998). Seismic anisotropy of oceanic upper mantle: Shear wave splitting methodologies and observations, *J. Geophys. Res.* **103**, no. B1, 749–771.

Geosciences Montpellier
Université de Montpellier II
34095 Montpellier, France
wueste@gm.univ-montp2.fr
bokelmann@gm.univ-montp2.fr

Manuscript received 19 September 2006.